BIOCHEMISTRY
including biophysical chemistry & molecular biology

Article

pubs.acs.org/biochemistry

Characterization of the Interdomain Motions in Hen Lysozyme Using Residual Dipolar Couplings as Replica-Averaged Structural Restraints in Molecular Dynamics Simulations

Alfonso De Simone,[†,‡] Rinaldo W. Montalvao,[†] Christopher M. Dobson,[†] and Michele Vendruscolo*[,†]

[†]Department of Chemistry, University of Cambridge, Cambridge CB2 1EW, United Kingdom

[‡]Division of Molecular Biosciences, Imperial College, London SW7 2AZ, United Kingdom

Supporting Information

ABSTRACT: Hen lysozyme is an enzyme characterized by the presence of two domains whose relative motions are involved in the mechanism of binding and release of the substrates. By using residual dipolar couplings as replica-averaged structural restraints in molecular dynamics simulations, we characterize the breathing motions describing the interdomain fluctuations of this protein. We found that the ensemble of conformations that we determined spans the entire range of structures of hen lysozyme deposited in the Protein Data Bank, including both the free and bound states, suggesting that the thermal motions in the free state provide access to the structures populated upon binding. The approach that we present illustrates how the use of residual dipolar couplings as replica-averaged structural restraints in molecular dynamics simulations makes it possible to explore conformational fluctuations of a relatively large amplitude in proteins.

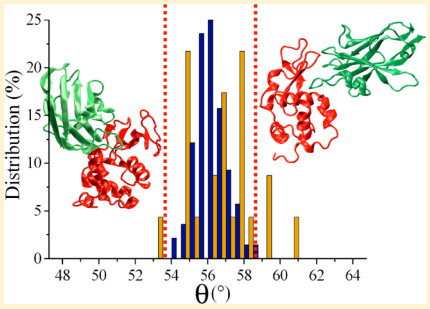

Protein molecules undergo complex conformational fluctuations on time scales ranging from picoseconds to seconds and beyond.[1−13] The accurate determination of such motions is key to understanding the biological properties of these molecules. In recent years, significant advances have been made toward this goal using nuclear magnetic resonance (NMR) spectroscopy.[5−18] Particularly promising results have been obtained by methods based on the analysis of residual dipolar couplings (RDCs),[19,20] which provide information on the structure and dynamics of proteins on the range of time scales relevant for biological processes.[9,16,21−23] Several methods have been proposed to use these parameters to derive structural ensembles representative of the dynamics of proteins.[24−30] The conformational fluctuations of ubiquitin have been determined through this approach,[24,25,27] enabling the molecular-recognition mechanism of this protein to be characterized.[27] In a related strategy, using RDCs as replica-averaged structural restraints in molecular dynamics simulations,[24,25] with the RDCs being calculated from the shape and charge[31−38] of each individual structure in the ensemble,[39,40] it has been possible to characterize the conformational substates populated by ribonuclease A in its native state.[39]

In this work, we apply this approach to characeterize the conformational fluctuations of hen lysozyme, an enzyme that catalyzes the hydrolysis of 1,4-β-linkages of cell-wall peptidoglycans[41] that has been studied by a range of different methods, including X-ray crystallography,[42−44] NMR spectroscopy,[45−47] and molecular dynamics simulations,[48,49] and whose native structure can be divided into two domains, an α domain (residues 1−38 and 86−130) and a β domain (residues 39−85) that contain primarily α-helical and β-sheet secondary structures, respectively.[42−44]

The method that we adopted here in which NMR parameters are used as replica-averaged structural restraints, which is an approach that has a long history in structural biology,[24,25,50−57] provides a convenient way to generate structural ensembles according to the maximum entropy principle and hence to translate experimental measurements into Boltzmann distributions that reveal the equilibrium properties of a protein molecule.[58−60]

METHODS

Molecular Dynamics Simulations with Replica-Averaged RDC Restraints. Molecular dynamics simulations with replica-averaged RDC restraints were implemented in the GROMACS package.[61] In this approach,[39,40] the structural information provided by RDC measurements is imposed to restrain the molecular dynamics simulations by adding a term, E_{RDC}, to a standard molecular mechanics force field, E_{MM}

$$E_{TOT} = E_{MM} + E_{RDC} \quad (1)$$

The resulting force field, E_{TOT}, is employed in the integration of the equations of motion. In this work, we used as E_{MM} the Amber99SB[62] force field, and the restraint term, E_{RDC}, is given by[24,25,29]

Received: June 12, 2013
Revised: August 12, 2013
Published: August 14, 2013

   dx.doi.org/10.1021/bi4007513 | *Biochemistry* 2013, 52, 6480−6486

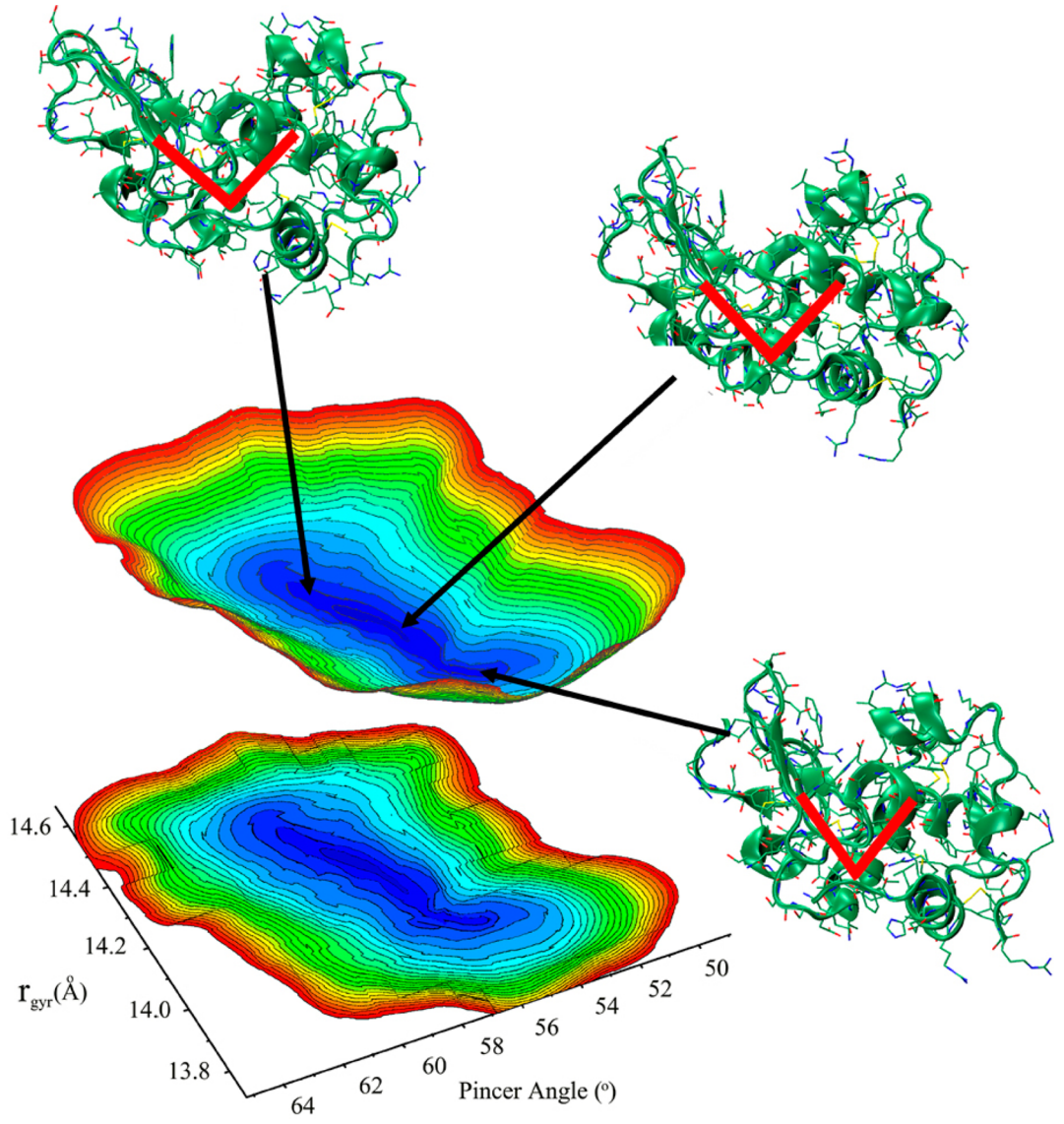

Figure 1. Free-energy landscape of hen lysozyme as a function of the radius of gyration, r_{gyr}, and the pincer angle, θ. The free energy is calculated as $F = -k_B T \log H(r_{gyr}, \theta)$, where T is the temperature, k_B is the Boltzmann constant, and H is the observed frequency of the values of r_{gyr} and θ sampled during the simulations. The pincer angle is calculated from the centers of mass of the Cα atoms from three protein regions: region 1 (in the α domain) spans residues 28−31 and 111−114, region 2 (in the hinge) spans residues 90−93, and region 3 (in the β domain) spans residues 44−45 and 51−52. Three representative structures characterized by large, intermediate, and small values of θ, respectively, are shown as ribbon diagrams. The pincer angle, θ, is shown on the structures as red chevrons.

$$E_{RDC} = \alpha \sum_i (D^{exp} - D^{calc})^2 \quad (2)$$

where α is the weight of the restraint term, and D^{exp} and D^{calc} are the experimental and calculated RDCs, respectively. The RDC of a given bond vector is calculated as[40]

$$D^{calc} = \frac{1}{M} \sum_{m=1}^{M} D_m \quad (3)$$

where m runs over the M replicas and D_m is the RDC of replica m, which is given by[40]

$$D = D_{max} \sum_{ij} \langle A_{ij} \rangle \cos \varphi_i \cos \varphi_j \quad (4)$$

where φ_i and φ_j are the angles between the internuclear vector and the molecular reference frame, i and j run over the three Cartesian coordinates, x, y, and z, and $\langle A_{ij} \rangle$ is the (i,j) component of the alignment tensor. The alignment tensor is calculated from the shape and charge of the protein molecule[31−38] using a procedure recently described.[39,40] We adopted such an approach here rather than the more commonly used singular value decomposition (SVD) method[63] because in the presence of conformational fluctuations of relatively large amplitude, such as those exhibited by hen lysozyme, the SVD method, when used in combination with the replica-averaging procedure of eqs 1−4, is less effective in capturing the motions of a protein.[39,40] The reason is that the SVD method does not necessarily provide the actual alignment tensor of a given structure but rather the alignment tensor that generates the RDC values in closest agreement with the experimental ones and hence is less well suited in describing the specific differences between the structures considered in the averaging procedure in eq 3.

dx.doi.org/10.1021/bi4007513 | *Biochemistry* 2013, 52, 6480−6486

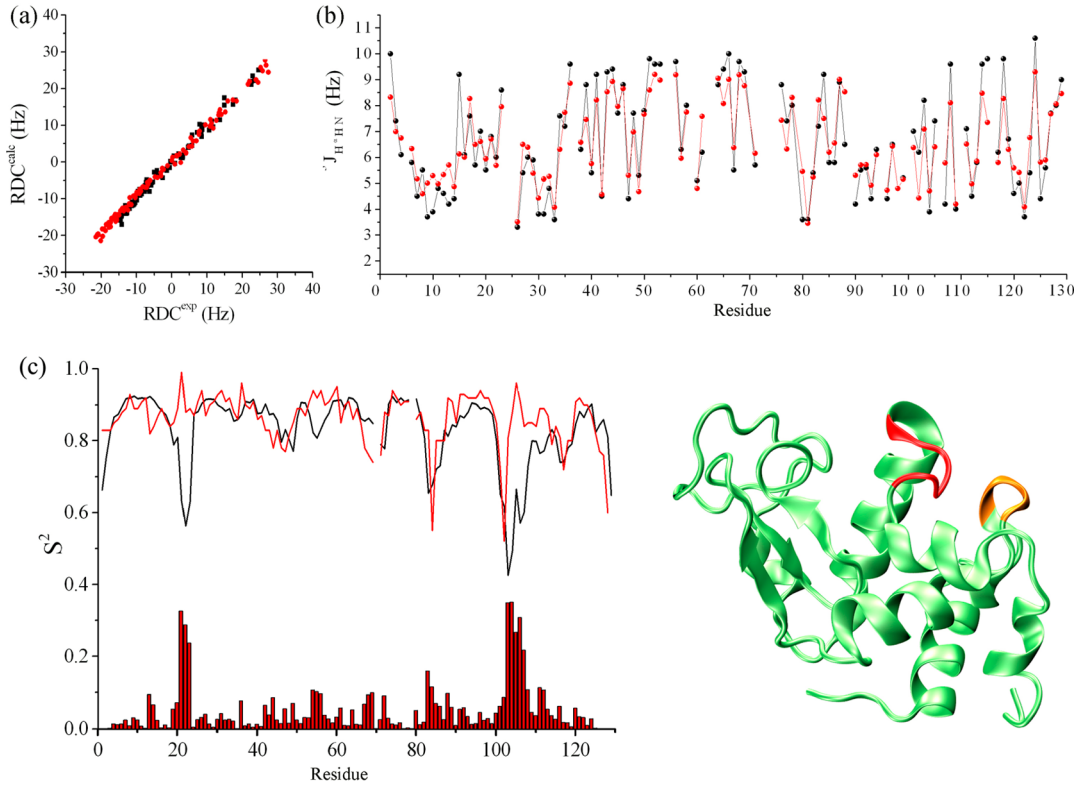

Figure 2. Validation of the hen lysozyme structural ensemble determined in this work. (a) Comparison of experimental and calculated RDCs. Black and red dots indicate RDCs measured in the presence of neutral and positively charged bicelles, respectively. The calculated RDCs match the experimental values with a Q factor of 0.09. (b) Comparison of experimental (black) and back-calculated (red) $^3J(H\alpha-HN)$ couplings. The standard deviation between the calculated and experimental value is 0.67 Hz. (c) Comparison of experimental (red line) and calculated (black line) S^2 order parameters. The absolute values of the differences of the sets of S^2 order parameters are shown at the bottom of the plot. Hen lysozyme is shown as a ribbon diagram with the regions of residues 21−23 (orange) and 103−107 (red) highlighted to indicate that they exhibit the largest deviations between the calculated and experimental S^2 order parameters. In these regions, the RDC ensemble described here captures the dynamics on the microsecond to millisecond time scales, in agreement with the large T1/T2 ratio of 4.18 for G22 (the mean ratio for the protein as a whole is 3.32).

The use of experimental measurements as replica-averaged structural restraints has the following justification.[58−60] Given the unavoidable approximations present in any given force field E_{MM}, an ensemble of structures generated by molecular dynamics simulations will not correspond to the true Boltzmann distribution of the system, which is unknown. Therefore, the calculation of the equilibrium value of any observable will provide results that will not match exactly the values measured experimentally. One can address this problem by using a given set of experimental measurements as replica-averaged structural restraints, which corresponds to making the minimal possible changes to the force field to obtain a match between the calculated and experimental values, at least for the specific set of measurements used as restraints. In this sense, the use of replica-averaged structural restraints represents an efficient maximum entropy method,[58−60] at least in the limit in which the number of replicas, M, and the weight, α, of the restraint term are very large.[58−60] As we have previously shown, it is possible to effectively achieve this limit even if the values of M and α remain relatively small and thus obtain conformational ensembles that provide a good agreement between experimental and calculated observables.[29,39,40,58] Following these procedures,[29,38−40] we used here $M = 16$ and for the weight, α, we first carried out an initial equilibration simulation at 300 K, during which the agreement between the calculated and experimental data was allowed to converge by gradually raising α to the largest possible value that did not generate numerical instabilities. Subsequently, we performed a series of 20 cycles of simulated annealing between 300 and 500 K to sample the conformational space. Each cycle was carried out for a total of 250 ps (125 000 molecular dynamics steps) with an integration step of 2 fs.

This approach has been shown to provide an accurate description of the conformational fluctuations of ubiquitin,[40] and it was further validated in the case of ribonuclease A, a protein with a two-domain structure (as is the one studied in the present work), by showing that the differences between two structural ensembles resulting from molecular dynamics simulations carried out with two different force fields could be essentially eliminated by imposing the RDCs back-calculated from the first ensemble as replica-averaged structural restraints in the molecular dynamics simulations with the second force field.[29]

RESULTS AND DISCUSSION

The structural ensemble of hen lysozyme that we have determined in this work, which was obtained using RDC data measured in charged and neutral bicelles,[47] illustrates how the thermal fluctuations of this protein are dominated by large breathing motions between its α and β domains. These motions can be described by the first eigenvector of the principal component analysis of the structural ensemble (Figure S1a). Indeed, the first and the second eigenvectors, which involve a twisting motion of the α domain (Figure S1b), represent more

dx.doi.org/10.1021/bi4007513 | Biochemistry 2013, 52, 6480−6486

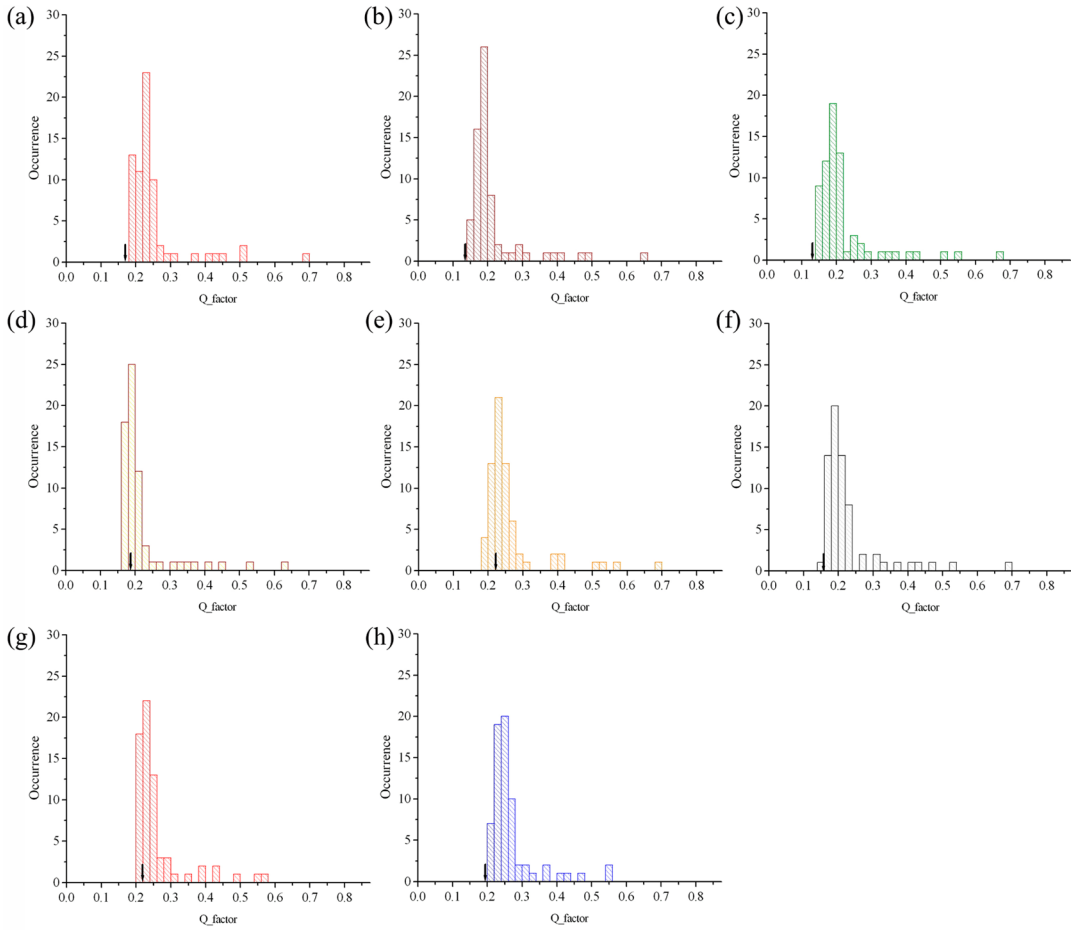

Figure 3. Validation of the hen lysozyme structural ensemble determined in this work using Q factors for N−H RDCs measured on seven independent alignment media that were not used as restraints in the simulations.[46] The distributions report individual Q factors obtained by fitting individual X-ray structures with the SVD method. In each panel, the arrows indicates the ensemble Q factor of our hen lysozyme ensemble. The Q factor values are (a) 0.171, (b) 0.142, (c) 0.138, (d) 0.184, (e) 0.221, (f) 0.159, (g) 0.219, and (e) 0.196. The alignment media are[46] (a) 7.5% esters/CTAB, (b) 5% esters, (c) ether/CTAB, (d) ether/La^{3+}, (e) CpBr/hex/NaBr, (f) C12E6/hex, (g) 7% acrylamide gel, and (h) Pf1.

than 70% of the overall backbone dynamics of the enzyme. Such collective motions, which influence the shape of the catalytic pocket located at their interface by altering the mutual orientation of the two domains, can be followed by defining a 'pincer' angle, θ, which is calculated from the centers of mass of Cα atoms from the α-domain, the hinge region, and the β-domain (Figure S2). The free energy projected onto the pincer angle, θ, and the radius of gyration presents a relatively broad basin (Figure 1), indicating that under the effect of thermal fluctuations the protein explores a relatively broad range of interdomain orientations on the millisecond time scale by rapidly interconverting between conformations and without crossing major free-energy barriers.

The hen lysozyme ensemble satisfies closely the RDCs that were used as restraints[47] (Q factor = 0.09, Figure 2a) as well as other sets of RDCs available from the literature[46] (Figure 3). As a further validation, the ^3J couplings back-calculated from the ensemble are in very good agreement with the corresponding experimental values,[64] with a standard deviation of only 0.66 Hz (Figure 2b). The calculated S^2 order parameters are in good agreement with the values determined from ^{15}N relaxation experiments[45] except for two spatially close regions on the protein (residues 21−23 and 103−107, Figure 2c,d).

These results suggest that such residues exhibit motions of significantly larger amplitude on the millisecond time scale compared to those on the nanosecond time scale monitored by the experimental S^2 values. The elevated T1/T2 ratio of residue G22 (4.18 on an average of 3.32 for the whole protein) are consistent with local dynamics on time scales of microseconds to milliseconds. These slow fluctuations are thus captured by the present RDC ensemble and are outside of the range of dynamics covered by ^{15}N relaxation experiments.

An analysis of the structures of ligand-free hen lysozyme available in the Protein Data Bank (Figure 4, blue histogram) provides a relatively narrow distribution of the pincer angle, θ (Figure 4b, green histogram). By contrast, the structures of the ligand-bound hen lysozyme in the Protein Data Bank cover a wider range of interdomain motions (Figure 4b, orange histogram). This difference may suggest an induced-fit mechanism[6] for protein recognition in which the binding process is associated with an alteration of the native conformational space of the protein in the free state. By considering, however, the distribution of the values of the pincer angles in the conformational ensemble that we determined in this work for the free state of hen lysozyme, one finds a range of values that cover all of those corresponding to the bound states, suggesting the presence of a conformational-selection mechanism[6,65] analogous to that previously observed for ubiquitin,[27] a protein characterized by conforma-

dx.doi.org/10.1021/bi4007513 | *Biochemistry* 2013, 52, 6480−6486

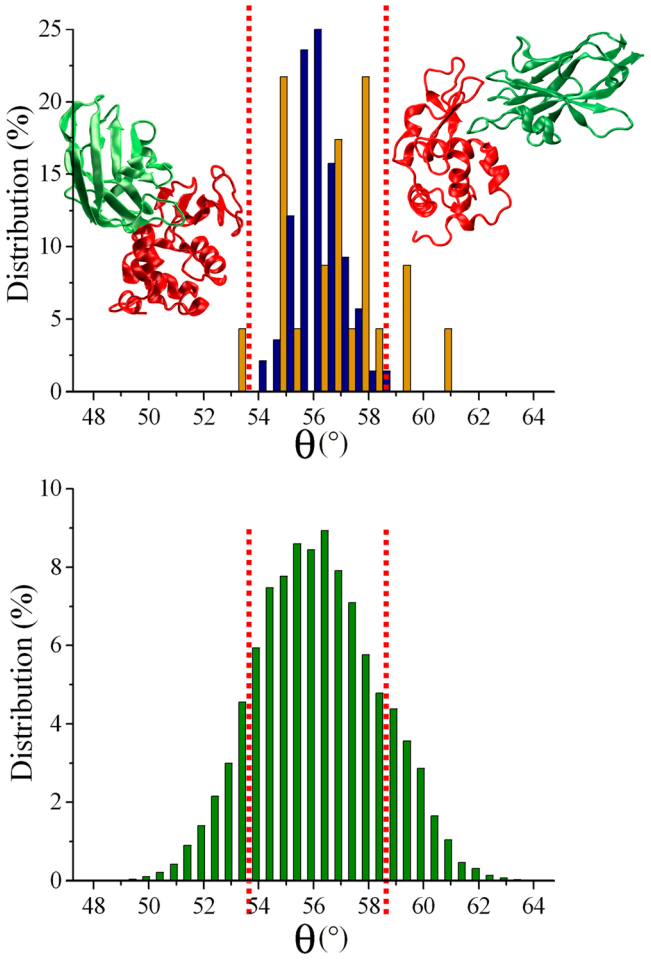

Figure 4. Characterization of the breathing motions in hen lysozyme. (a) Comparison of distributions of the pincer angle, θ, for the two sets of structures of lysozyme available in the Protein Data Bank (PDB), representing the free (blue) and bound (orange) states, respectively. Dashed red lines highlight three zones with small, intermediate, and large values of the pincer angle, θ. The free structures in the PDB populate only the intermediate angles, whereas the bound structures in the PDB populate also small and large angles. Representative protein complexes (1ri8 and 1zmy) of hen lysozyme are shown by red and green ribbons for hen lysozyme and the binding partners, respectively. (b) Distribution of the angle θ in the ensemble of conformations representing the free state of hen lysozyme, as determined in this work using RDCs as replica-averaged structural restraints in molecular dynamics simulations. The dashed red lines are the same as in panel a.

tional fluctuations of considerably smaller amplitude than those considered here.

CONCLUSIONS

We have described a procedure to incorporate RDC data as replica-averaged structural restraints in molecular dynamics simulations to determine a highly heterogeneous conformational ensemble of a protein. Although the present investigation has been focused on the conformational properties of hen lysozyme, the method that we have discussed is general and can be used to study the equilibrium dynamics of other proteins on the millisecond time scale. This type of approach should therefore be capable of providing an accurate representation of the conformational fluctuations of a variety of proteins in solution under a range of different conditions.

ASSOCIATED CONTENT

Supporting Information

Principal component analysis of the hen lysozyme ensemble and definition of the pincer angle θ of hen lysozyme. This material is available free of charge via the Internet at http://pubs.acs.org.

AUTHOR INFORMATION

Corresponding Author

*E-mail: mv245@cam.ac.uk; Tel: +44-1223-763873.

Funding

This work was supported by grants from the EPSRC (A.D.S.), EMBO (A.D.S.), Marie Curie (A.D.S.), and BBSRC (R.W.M. and M.V.).

Notes

The authors declare no competing financial interest.

REFERENCES

(1) Frauenfelder, H., Sligar, S. G., and Wolynes, P. G. (1991) The energy landscapes and motions of proteins. *Science 254*, 1598−1603.
(2) Fersht, A. R. (1999) *Structure and Mechanism in Protein Science: A Guide to Enzyme Catalysis and Protein Folding*, W. H. Freeman, New York.
(3) Karplus, M., and Kuriyan, J. (2005) Molecular dynamics and protein function. *Proc. Natl. Acad. Sci. U.S.A. 102*, 6679−6685.
(4) Dobson, C. M., Sali, A., and Karplus, M. (1998) Protein folding: A perspective from theory and experiment. *Angew. Chem., Int. Ed. 37*, 868−893.
(5) Baldwin, A. J., and Kay, L. E. (2009) NMR spectroscopy brings invisible protein states into focus. *Nature Chem. Biol. 5*, 808−814.
(6) Boehr, D. D., Nussinov, R., and Wright, P. E. (2009) The role of dynamic conformational ensembles in biomolecular recognition. *Nat. Chem. Biol. 5*, 789−796.
(7) Bouvignies, G., Vallurupalli, P., Hansen, D. F., Correia, B. E., Lange, O., Bah, A., Vernon, R. M., Dahlquist, F. W., Baker, D., and Kay, L. E. (2011) Solution structure of a minor and transiently formed state of a T4 lysozyme mutant. *Nature 477*, 111−114.
(8) Guerry, P., Salmon, L., Mollica, L., Roldan, J. L. O., Markwick, P., van Nuland, N. A. J., McCammon, J. A., and Blackledge, M. (2013) Mapping the population of protein conformational energy sub-states from NMR dipolar couplings. *Angew. Chem., Int. Ed. 52*, 3181−3185.
(9) Kalodimos, C. G. (2011) NMR reveals novel mechanisms of protein activity regulation. *Protein Sci. 20*, 773−782.
(10) Korzhnev, D. M., Religa, T. L., Banachewicz, W., Fersht, A. R., and Kay, L. E. (2010) A transient and low-populated protein-folding intermediate at atomic resolution. *Science 329*, 1312−1316.
(11) Lorieau, J. L., Louis, J. M., Schwieters, C. D., and Bax, A. (2012) pH-Triggered, activated-state conformations of the influenza hemagglutinin fusion peptide revealed by NMR. *Proc. Natl. Acad. Sci. U.S.A. 109*, 19994−19999.
(12) Marsh, J. A., Teichmann, S. A., and Forman-Kay, J. D. (2012) Probing the diverse landscape of protein flexibility and binding. *Curr. Opin. Struct. Biol. 22*, 643−650.
(13) Neudecker, P., Robustelli, P., Cavalli, A., Walsh, P., Lundstrom, P., Zarrine-Afsar, A., Sharpe, S., Vendruscolo, M., and Kay, L. E. (2012) Structure of an intermediate state in protein folding and aggregation. *Science 336*, 362−366.
(14) Boehr, D. D., McElheny, D., Dyson, H. J., and Wright, P. E. (2006) The dynamic energy landscape of dihydrofolate reductase catalysis. *Science 313*, 1638−1642.
(15) Henzler-Wildman, K. A., Lei, M., Thai, V., Kerns, S. J., Karplus, M., and Kern, D. (2007) A hierarchy of timescales in protein dynamics is linked to enzyme catalysis. *Nature 450*, 913−916.
(16) Mittermaier, A., and Kay, L. E. (2006) New tools provide new insights in NMR studies of protein dynamics. *Science 312*, 224−228.

(17) Palmer, A. G. (2004) NMR characterization of the dynamics of biomacromolecules. *Chem. Rev. 104*, 3623−3640.
(18) Vendruscolo, M., and Dobson, C. M. (2006) Dynamic visions of enzymatic reactions. *Science 313*, 1586−1587.
(19) Tjandra, N., and Bax, A. (1997) Direct measurement of distances and angles in biomolecules by NMR in a dilute liquid crystalline medium. *Science 278*, 1111−1114.
(20) Tolman, J. R., Flanagan, J. M., Kennedy, M. A., and Prestegard, J. H. (1997) NMR evidence for slow collective motions in cyanometmyoglobin. *Nat. Struct. Biol. 4*, 292−297.
(21) Bax, A. (2003) Weak alignment offers new NMR opportunities to study protein structure and dynamics. *Protein Sci. 12*, 1−16.
(22) Blackledge, M. (2005) Recent progress in the study of biomolecular structure and dynamics in solution from residual dipolar couplings. *Prog. Nucl. Magn. Reson. Spectrosc. 46*, 23−61.
(23) Meiler, J., Prompers, J. J., Peti, W., Griesinger, C., and Bruschweiler, R. (2001) Model-free approach to the dynamic interpretation of residual dipolar couplings in globular proteins. *J. Am. Chem. Soc. 123*, 6098−6107.
(24) Clore, G. M., and Schwieters, C. D. (2004) Amplitudes of protein backbone dynamics and correlated motions in a small alpha/beta protein: Correspondence of dipolar coupling and heteronuclear relaxation measurements. *Biochemistry 43*, 10678−10691.
(25) Clore, G. M., and Schwieters, C. D. (2004) How much backbone motion in ubiquitin is required to account for dipolar coupling data measured in multiple alignment media as assessed by independent cross-validation? *J. Am. Chem. Soc. 126*, 2923−2938.
(26) Bouvignies, G., Markwick, P., Bruscheweiler, R., and Blackledge, M. (2006) Simultaneous determination of protein backbone structure and dynamics from residual dipolar couplings. *J. Am. Chem. Soc. 128*, 15100−15101.
(27) Lange, O. F., Lakomek, N. A., Fares, C., Schroder, G. F., Walter, K. F. A., Becker, S., Meiler, J., Grubmuller, H., Griesinger, C., and de Groot, B. L. (2008) Recognition dynamics up to microseconds revealed from an RDC-derived ubiquitin ensemble in solution. *Science 320*, 1471−1475.
(28) Showalter, S. A., and Bruschweiler, R. (2007) Quantitative molecular ensemble interpretation of NMR dipolar couplings without restraints. *J. Am. Chem. Soc. 129*, 4158−4159.
(29) De Simone, A., Richter, B., Salvatella, X., and Vendruscolo, M. (2009) Toward an accurate determination of free energy landscapes in solution states of proteins. *J. Am. Chem. Soc. 131*, 3810−3811.
(30) Huang, J. R., and Grzesiek, S. (2010) Ensemble calculations of unstructured proteins constrained by RDC and PRE data: A case study of urea-denatured ubiquitin. *J. Am. Chem. Soc. 132*, 694−705.
(31) Zweckstetter, M., and Bax, A. (2000) Prediction of sterically induced alignment in a dilute liquid crystalline phase: Aid to protein structure determination by NMR. *J. Am. Chem. Soc. 122*, 3791−3792.
(32) Almond, A., and Axelsen, J. B. (2002) Physical interpretation of residual dipolar couplings in neutral aligned media. *J. Am. Chem. Soc. 124*, 9986−9987.
(33) Azurmendi, H. F., and Bush, C. A. (2002) Tracking alignment from the moment of inertia tensor (tramite) of biomolecules in neutral dilute liquid crystal solutions. *J. Am. Chem. Soc. 124*, 2426−2427.
(34) Berlin, K., O'Leary, D. P., and Fushman, D. (2009) Improvement and analysis of computational methods for prediction of residual dipolar couplings. *J. Magn. Reson. 201*, 25−33.
(35) Fernandes, M. X., Bernado, P., Pons, M., and de la Torre, J. G. (2001) An analytical solution to the problem of the orientation of rigid particles by planar obstacles. Application to membrane systems and to the calculation of dipolar couplings in protein NMR spectroscopy. *J. Am. Chem. Soc. 123*, 12037−12047.
(36) Ferrarini, A. (2003) Modeling of macromolecular alignment in nematic virus suspensions. Application to the prediction of NMR residual dipolar couplings. *J. Phys. Chem. B 107*, 7923−7931.
(37) van Lune, F., Manning, L., Dijkstra, K., Berendsen, H. J. C., and Scheek, R. M. (2002) Order-parameter tensor description of hpr in a medium of oriented bicelles. *J. Biomol. NMR 23*, 169−179.
(38) Zweckstetter, M. (2008) NMR: Prediction of molecular alignment from structure using the pales software. *Nat. Protoc. 3*, 679−690.
(39) De Simone, A., Montalvao, R. W., and Vendruscolo, M. (2011) Determination of conformational equilibria in proteins using residual dipolar couplings. *J. Chem. Theory Comput. 7*, 4189−4195.
(40) Montalvao, R. W., De Simone, A., and Vendruscolo, M. (2011) Determination of structural fluctuations of proteins from structure-based calculations of residual dipolar couplings. *J. Biomol. NMR 53*, 281−292.
(41) Phillips, D. C. (1967) Hen egg-white lysozyme molecule. *Proc. Natl. Acad. Sci. U.S.A. 57*, 484−495.
(42) Blake, C. C. F., Koenig, D. F., Mair, G. A., North, A. C. T., Phillips, D. C., and Sarma, V. R. (1965) Structure of hen egg-white lysozyme. A three-dimensional Fourier synthesis at 2 Angstrom resolution. *Nature 206*, 757−761.
(43) Walsh, M. A., Schneider, T. R., Sieker, L. C., Dauter, Z., Lamzin, V. S., and Wilson, K. S. (1998) Refinement of triclinic hen egg-white lysozyme at atomic resolution. *Acta Crystallogr., Sect. D 54*, 522−546.
(44) Artymiuk, P. J., and Blake, C. C. F. (1981) Refinement of human lysozyme at 1.5 a resolution analysis of nonbonded and hydrogen-bond interactions. *J. Mol. Biol. 152*, 737−762.
(45) Buck, M., Boyd, J., Redfield, C., Mackenzie, D. A., Jeenes, D. J., Archer, D. B., and Dobson, C. M. (1995) Structural determinants of protein dynamics: Analysis of ^{15}N NMR relaxation measurements for main-chain and side-chain nuclei of hen egg-white lysozyme. *Biochemistry 34*, 4041−4055.
(46) Higman, V. A., Boyd, J., Smith, L. J., and Redfield, C. (2011) Residual dipolar couplings: Are multiple independent alignments always possible? *J. Biomol. NMR 49*, 53−60.
(47) Schwalbe, H., Grimshaw, S. B., Spencer, A., Buck, M., Boyd, J., Dobson, C. M., Redfield, C., and Smith, L. J. (2001) A refined solution structure of hen lysozyme determined using residual dipolar coupling data. *Protein Sci. 10*, 677−688.
(48) Smith, L. J., Mark, A. E., Dobson, C. M., and van Gunsteren, W. F. (1995) Comparison of md simulations and NMR experiments for hen lysozyme. Analysis of local fluctuations, cooperative motions, and global changes. *Biochemistry 34*, 10918−10931.
(49) Soares, T. A., Daura, X., Oostenbrink, C., Smith, L. J., and van Gunsteren, W. F. (2004) Validation of the gromos force-field parameter set 45α3 against nuclear magnetic resonance data of hen egg lysozyme. *J. Biomol. NMR 30*, 407−422.
(50) Fennen, J., Torda, A. E., and van Gunsteren, W. F. (1995) Structure refinement with molecular-dynamics and a Boltzmann-weighted ensemble. *J. Biomol. NMR 6*, 163−170.
(51) Kessler, H., Griesinger, C., Lautz, J., Muller, A., van Gunsteren, W. F., and Berendsen, H. J. C. (1988) Conformational dynamics detected by nuclear magnetic-resonance NOE values and J coupling constants. *J. Am. Chem. Soc. 110*, 3393−3396.
(52) Torda, A. E., Scheek, R. M., and van Gunsteren, W. F. (1989) Time-dependent distance restraints in molecular-dynamics simulations. *Chem. Phys. Lett. 157*, 289−294.
(53) Torda, A. E., Scheek, R. M., and van Gunsteren, W. F. (1990) Time-averaged nuclear Overhauser effect distance restraints applied to tendamistat. *J. Mol. Biol. 214*, 223−235.
(54) Bonvin, A., Boelens, R., and Kaptein, R. (1994) Time-averaged and ensemble-averaged direct noe restraints. *J. Biomol. NMR 4*, 143−149.
(55) Bonvin, A., and Brunger, A. T. (1995) Conformational variability of solution nuclear-magnetic-resonance structures. *J. Mol. Biol. 250*, 80−93.
(56) Kemmink, J., and Scheek, R. M. (1995) Dynamic modeling of a helical peptide in solution using NMR data: Multiple conformations and multi-spin effects. *J. Biomol. NMR 6*, 33−40.
(57) Lee, J., Chen, J. H., Brooks, C. L., and Im, W. P. (2008) Application of solid-state NMR restraint potentials in membrane protein modeling. *J. Magn. Reson. 193*, 68−76.
(58) Cavalli, A., Camilloni, C., and Vendruscolo, M. (2013) Molecular dynamics simulations with replica-averaged structural

restraints generate structural ensembles according to the maximum entropy principle. *J. Chem. Phys. 138*, 094112-1−094112-5.
(59) Pitera, J. W., and Chodera, J. D. (2012) On the use of experimental observations to bias simulated ensembles. *J. Chem. Theory Comput. 8*, 3445−3451.
(60) Roux, B., and Weare, J. (2013) On the statistical equivalence of restrained-ensemble simulations with the maximum entropy method. *J. Chem. Phys. 138*, 084107-1−084107-8.
(61) Hess, B., Kutzner, C., van der Spoel, D., and Lindahl, E. (2008) Gromacs 4: Algorithms for highly efficient, load-balanced, and scalable molecular simulation. *J. Chem. Theory Comput. 4*, 435−447.
(62) Hornak, V., Abel, R., Okur, A., Strockbine, B., Roitberg, A., and Simmerling, C. (2006) Comparison of multiple amber force fields and development of improved protein backbone parameters. *Proteins 65*, 712−725.
(63) Losonczi, J. A., Andrec, M., Fischer, M. W. F., and Prestegard, J. H. (1999) Order matrix analysis of residual dipolar couplings using singular value decomposition. *J. Magn. Reson. 138*, 334−342.
(64) Smith, L. J., Sutcliffe, M. J., Redfield, C., and Dobson, C. M. (1991) Analysis of phi and chi-1 torsion angles for hen lysozyme in solution from proton NMR spin-spin coupling constants. *Biochemistry 30*, 986−996.
(65) Tsai, C. J., Kumar, S., Ma, B. Y., and Nussinov, R. (1999) Folding funnels, binding funnels, and protein function. *Protein Sci. 8*, 1181−1190.